

## Simulation of polymers in a curved box: Variable range bonding models

Y.Y. SUZUKI<sup>1</sup>(\*), T. DOTERA<sup>2</sup> and M. HIRABAYASHI<sup>2</sup>

<sup>1</sup> *NTT Basic Research Laboratories, Atsugi 243-0198, Japan*

<sup>2</sup> *Saitama Study Center, the University of the Air, 682-2 Nishiki-cho, Omiya 331-0851, Japan*

(received ; accepted )

PACS. 36.20-r – Macromolecules and polymer molecules.

PACS. 05.10Ln – Monte Carlo methods.

PACS. 82.65Pa – Surface-enhanced molecular states and other gas-surface interactions.

**Abstract.** – We propose new polymer models for Monte Carlo simulation and apply them to a polymer chain confined in a relatively thin box which has both curved and flat sides, and show that either an ideal or an excluded-volume chain spends more time in the curved region than in the flat region. The ratio of the probability of finding a chain in the curved region and in flat region increases exponentially with increasing chain length. The results for ideal chains are quantitatively consistent with a previously published theory. We find that the same effect appears with excluded-volume chains and a similar scaling relation can be applied to them up to a certain length of the polymer.

*Introduction.* – The structure [1], [2], [3], [4] and dynamics [5], [6], [7] of polymer chains confined within a narrow space such as in a slit (Fig. 1) are important for practical applications, e.g. filtration, gel permeation chromatography and oil recovery, and have attracted much interest. [8] The effect of confinement on polymer chains was calculated theoretically in well-defined geometries (a slit and a tube) and was simulated by a lattice model [9] and an off-lattice model. [10]

Recently, polymer confinement in curved boxes (a cylindrical shell, an undulated slit, etc) was studied. [11], [12] Such studies can relate to not only the behaviour of polymers confined in complex rigid geometries but also the behaviour of deformable bilayer membranes confining the polymer chains.

Yaman *et al.* [11] showed that an ideal (Gaussian) polymer chain confined between cylindrical shells (Fig. 2) has a lower free energy than one confined between two flat surfaces (Fig. 1), and predicted that polymer chains confined in bilayer membranes reduce the effective bending rigidity of the membranes and might induce spontaneous curvature in the system, e.g. leading to transitions from lamellar to bicontinuous phases.

---

(\*) E-mail address: suzuki@bri.ntt.co.jp

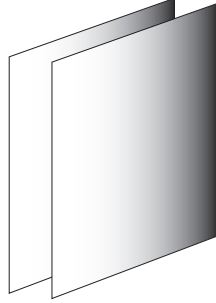


Fig. 1. – flat box



Fig. 2. – cylindrical shell

Above mentioned studies of the confinement effects are limited to ideal chains. The ideal chain represents the polymers in  $\Theta$  solvents where the excluded-volume interactions are compensated for by monomer-monomer interactions. It can act as an unperturbed model for a perturbation calculation of the “real” chain in a good solvent characterized by excluded-volume interactions. However, the perturbation calculation is difficult for confined flexible polymers and few publications have addressed the excluded-volume effects. [13]

In this paper, we investigate both curved surface effects and excluded-volume effects on a flexible polymer confined between two surfaces using Monte Carlo simulations and compare with an ideal chain confined in the same geometry. We suppose that the surfaces are purely repulsive (no trend towards adsorption), with and without excluded-volume interactions. In particular, we are interested in the polymer behaviour when the polymer chain has a large size relative to the gap between the confining surfaces. The effect is sensitive to the curvature of the surfaces, therefore, our off-lattice simulation has the strong advantage over a lattice simulation where the curved surface is described by a zig-zag boundary (steps of flat surface strips).

First, we review the analytical study for ideal chains by Yaman *et al.* [11] Next, we propose new simulation models and check our algorithms in the free  $n$ -dimensional spaces to see if the models reproduce the known characteristics of flexible polymers. Then, we apply our simulation to ideal chains confined in a race-track box composed of curved and flat regions (Fig. 3) in order to compare with the analytical results by Yaman *et al.* Finally, we apply our simulation to excluded-volume chains confined to the race-track box.

*Analytical study for ideal chains by Yaman et al.* – For a random walk of  $N$  steps with

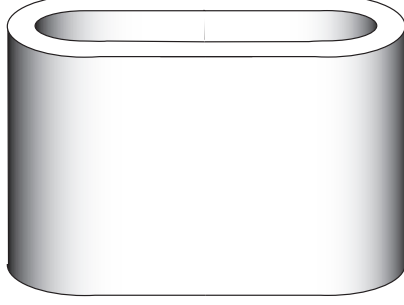


Fig. 3. – race-track box

endpoints at  $r$  and  $r'$ , the propagator  $G(r, r', N)$  is defined as [8]

$$\left( \frac{\partial}{\partial N} - \frac{l^2}{6} \nabla_r^2 \right) G(r, r', N) = \delta(r - r') \delta(N), \quad (1)$$

where  $l$  is the length of one step. The ideal chain is modelled as a random walk in space, where  $l$  and  $N$  correspond to the characteristic length of a monomer and the degree of polymerizations, respectively.

The partition function is a sum over all configurations:

$$Z = \frac{1}{V} \int dr dr' G(r, r', N). \quad (2)$$

With the eigenfunction expansion:

$$G(r, r', N) = \sum_n \Psi_n^*(r) \Psi_n(r') e^{-NE_n l^2/6} \Theta(N), \quad (3)$$

where  $\Theta(N)$  is the step function, our problem of a polymer confined in a spherical annulus in arbitrary space dimension  $D$  with radius  $a$  and thickness  $d$  reduces to

$$\nabla^2 \Psi(r) = -E \Psi(r), \quad (4)$$

under SO( $D$ ) symmetry and the boundary conditions:

$$\Psi(|r| = a) = \Psi(|r| = a + d) = 0. \quad (5)$$

For the radial wave function:

$$\left\{ \frac{d^2}{du^2} + (D-1) \frac{1}{u} \frac{d}{du} + \epsilon - \frac{\xi^2}{u^2} \right\} \Phi_\nu(u) = 0, \quad (6)$$

where  $\epsilon = Ed^2$ ,  $\xi^2 = \nu^2 + (D-2)^2/2$ , and  $u = r/d$ , the boundary conditions are  $\Phi_\nu(\eta) = \Phi_\nu(\eta+1) = 0$ , where  $\eta = a/d$ . The general solution of Eq.(6) is

$$\Phi_\nu(u) = AJ_\xi(\sqrt{\epsilon}u) + BN_\xi(\sqrt{\epsilon}u), \quad (7)$$

where  $J$  and  $N$  are the standard Bessel functions. The boundary condition determines the relation between  $\epsilon$  and  $\eta$ . For spherical symmetry, only  $\nu = 0$  states contribute to the partition function. We label these  $s$ -wave states by  $n = 1, 2, \dots$ , and define the normalized radial wave function as  $R_n(r)$  for  $\nu = 0$ .

For a spherical annulus with a large inner radius  $a$  and a small thickness  $d$ ,  $E_n$  can be obtained perturbationally:

$$E_n(a, d) = \left(\frac{n\pi}{d}\right)^2 + \frac{(D-1)(D-3)}{4d^2} \left[ \left(\frac{d}{a}\right)^2 - \left(\frac{d}{a}\right)^3 + \left(\frac{d}{a}\right)^4 \left(1 - \frac{3}{8n^2\pi^2}\right) + \dots \right]. \quad (8)$$

Note that  $D = 1$  is a slit between two flat surfaces (Fig. 1),  $D = 2$  is a cylindrical shell (Fig. 2),  $D = 3$  is a spherical shell. The curvature lowers the spherically symmetric energy spectrum for  $1 < D < 3$ .

The partition function becomes

$$Z = \frac{1}{V} \sum_{n=1}^{\infty} e^{-NE_n(a,d)l^2/6} \left| \int dr r^{(D-1)} R_n(r) \right|^2. \quad (9)$$

To indicate explicitly the dependence of the energies on  $a$  and  $d$ , we introduce  $B_n(a, d)$ :

$$B_n(a, d) \equiv \frac{\left| \int dr r^{(D-1)} R_n(r) \right|^2}{\frac{S_{D-1}}{D} \{(a+d)^D - a^D\}} \quad (10)$$

where  $S_D$  is the surface area of the unit sphere in  $D$ -dimensional space. The free energy is then given by

$$F = -kT \ln \left[ \sum_{n=1}^{\infty} B_n(a, d) e^{-E_n(a,d)Nl^2/6} \right]. \quad (11)$$

In this paper, we are interested in the case of a cylindrical shell ( $D = 2$ ) in three dimensions, for a polymer size  $R_g \sim \sqrt{N}l$  larger than the shell thickness  $d$ . Then, the leading term of the free energy difference between the cylindrical shell and the flat box ( $D = 1$ ) is

$$\Delta F \sim kT (E_1|_{D=2} - E_1|_{D=1}) \frac{Nl^2}{6} = -kTN \frac{l^2}{24a^2}. \quad (12)$$

From this result, Yaman *et al.* predicted that confining an ideal polymer chain into the bilayer membrane lowers the effective bending rigidity of the membrane and might induce spontaneous symmetry breaking of the membrane. Another interpretation of this result is that a polymer chain confined in the rigid shell is attracted into curved region, and that the ratio of probability finding a polymer chain in equivalent volume of curved and flat regions should be

$$C = e^{-\Delta F/kT} = \exp\left(\frac{Nl^2}{24a^2}\right). \quad (13)$$

Here, we assume that the size of the confined polymer is smaller than the characteristic length of the curved and flat sections.

*Models and method.* – Our polymer simulations are off-lattice beads and bonds models with  $N + 1$  beads and  $N$  bonds; they are relaxed versions of the random flight model with variable bond lengths. We call this the variable range bonding model. The models consist of the following conditions: (1) Connectivity:  $|\mathbf{r}_i - \mathbf{r}_{i+1}| \leq 1.0$ , where  $\mathbf{r}_i = (r_{i1}, r_{i2}, \dots, r_{in})$  stands for the position of the  $i$ -th bead. (2) Excluded-volume:  $|\mathbf{r}_i - \mathbf{r}_j| \geq 2r_e$ , for all  $i, j$ .  $r_e$  is the radius of the excluded volume of the beads. (3) Geometric constraint: the beads are in a confining geometry, here a race-track box (Fig. 3). Note that we impose the last condition

only on beads, but not on bonds. Thus, we even allow a bond that cuts through the curved wall as long as two beads attached to the bond satisfy the geometric constraint. We consider two models: Model-I which requires (1) and (3), and Model-E which requires (1)–(3). They correspond to the ideal polymer and the excluded-volume polymer respectively.

Our Monte Carlo (MC) algorithm is the following. i) Select a bead at random. ii) Generate a trial jump:  $\mathbf{r} \rightarrow \mathbf{r} + \mathbf{\Delta}$ . Each component of the jump vector  $\Delta_\mu$  ( $\mu = 1, 2, \dots, n$ ) is independently determined by the Gaussian distribution with zero mean value and a standard deviation of 0.3 for Model-I and 0.15 for Model-E. The Gaussian distribution is generated by the Box-Muller method. [14] iii) Check if the new position satisfies above mentioned conditions: (1) and (3) for Model-I, (1)–(3) for Model-E; if it does, accept the jump; if not, abandon the jump. iv) Return to i). For a simulation with  $N + 1$  beads,  $N + 1$  cycles comprise one MC step.

The reason to halve the standard deviation of the Gaussian distribution of the jump distance for Model-E is to increase the acceptance ratio of the bead jump although the bead in Model-E is restricted by the excluded-volume interactions compared with Model-I.

For Model-I in free  $n$ -dimensional space, the bond distribution is expected to be uniform inside the  $n$ -dimensional sphere with radius 1. Therefore, the bond length distribution is described by the distribution function  $P(r)$  of bond length  $r$  for  $0 \leq r \leq 1$  as

$$P(r) = nr^{n-1}, \quad (14)$$

and

$$\int_0^1 P(r)dr = 1. \quad (15)$$

Thus, the mean bond lengths are analytically calculated as

$$\int_0^1 r^2 P(r)dr = n/(n+2), \quad (16)$$

and the chain should be a Gaussian chain with bond length  $\sqrt{n/(n+2)}$ . The mean square end-to-end distance is analytically calculated as  $\langle R_N^2 \rangle = Nn/(n+2)$ . For 3-dimensions, the mean square bond length becomes  $\langle l^2 \rangle = 0.6$ . To evaluate the mean square end-to-end distances  $\langle R_N^2 \rangle$  by simulations, we made ten runs of simulation with  $4 \times 10^6$  MC steps for each length up to 200 beads. The simulation results are linearly fit by:  $\langle R_N^2 \rangle = 0.334N$  in 1D,  $0.492N$  in 2D,  $0.594N$  in 3D, which implies that  $\langle l^2 \rangle = 0.594$  for 3-dimensions. They are consistent with the analytical calculations.

For Model-E in the free  $n$ -dimensional space, we also carried out a series of simulations with  $4 \times 10^6$  MC steps. We plot the results for free 3-dimensional space in Fig. 4. The fitting exponent  $\nu = 0.601$  matches the best theoretical evaluation  $\nu = 0.588$  with 2 % error. The square average of the bond length is obtained as  $\langle l^2 \rangle = 0.6742$ .

Our race-track geometry (Fig. 3) consists of two flat sections and two curved sections. The width of the track is  $d = 0.5$ , the radius of the inside wall of the curved sections is  $a = 4.75$ , and the length of the flat sections is  $L = 15.71$ . The volume of the curved region and the flat region are the same.

For race-track simulations of Model-E, we use the same geometry as used for the Model-I, except that the width of the race-track  $d = 0.5$  is defined relative to the center of the beads. When the width is defined relative to the surface of the beads, it is  $d + 2r_e = 1.0$  and the radius of the inside wall is  $a - r_e = 4.5$  where  $r_e = 0.25$  is the radius of the beads.

To avoid localization on one side of the track, the polymer is relocated, every  $10^6$  MC steps, to the position of  $180^\circ$  rotation with respect to the center point of the track. The position data

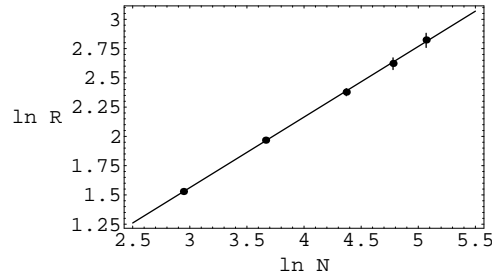


Fig. 4. – Log-log plot of the end-to-end distance of Model-E in free 3D space. The fitting curve is  $R \propto N^{0.601}$ .

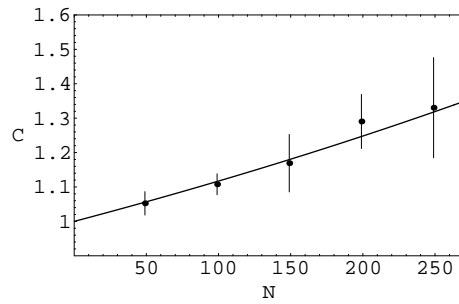


Fig. 5. – Results of Model-I. The line is drawn according to the theoretical curve with parameters  $a = 4.75$ ,  $\langle l^2 \rangle = 0.6$ :  $C = \exp(N/902.5)$ .

of beads are gathered every 1000 MC steps. Such data give us an idea of a density profile of the polymer in the restricted geometry. We divide the number of beads recorded in the curved region by the number of beads recorded in the flat region to obtain the probability ratio  $C$ .

The advantages of our polymer models are 1) the movement of polymer in the narrow space is facilitated due to variable bond lengths and variable range bead jumping, and 2) the high probability of polymer approaching to the wall compared to models with fixed bond length and fixed range bead jumping is convenient to observe the effects in proximity to the curved wall.

*Results and discussions.* – For each model and each polymer length, we carried out 5 runs of simulation with  $4 \times 10^8$  MC steps after an initial randomized stage ( $10^6$  MC steps).

For Model-I, the race-track simulation is performed for each chain length (number of beads) :  $N + 1 = 50, 100, 150, 200, 250$ . The results are plotted by in Fig. 5. The geometry gives parameters:  $d = 0.5$  and  $a = 4.75$ . The mean square of the bond length is analytically calculated as  $\langle l^2 \rangle = 0.6$ . Then, the theoretical curve with the parameters is given by  $C = \exp(N/902.5)$ .

For Model-E, the race-track simulation is performed for each chain length:  $N + 1 = 25, 50, 75, 100, 125$ . The results are plotted in Fig. 6. We try to fit the data of the excluded-volume chains by the theoretical curve developed by Yaman *et al.* for the Gaussian chain. The geometry gives parameters:  $d = 1.0$  and  $a = 4.5$ . The mean square of the bond length is evaluated by our free space simulations as  $\langle l^2 \rangle = 0.6742$ . Then, the theoretical curve with the parameters

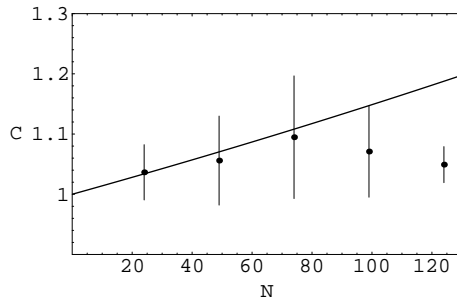


Fig. 6. – Results of Model-E. The line is drawn according to the theoretical curve for a Gaussian chain with parameters  $a = 4.5$ ,  $\langle l^2 \rangle = 0.6742$ :  $C = \exp(N/720.9)$ .

is given by  $C = \exp(N/947.5)$ .

In Model-I, our simulation results (Fig. 5) fit the analytical formula developed by Yaman *et al.* for all the chain lengths. In Model-E, our results (Fig. 6) are well described by the same formula as far as the chain lengths are short, however, they show a deviation when the chain gets longer.

The excluded-volume effects result in a elongated equilibrium polymer shape compared with the ideal chain. This is confirmed by the snap shots of our simulations. They show that the length of the excluded-volume chain with  $N + 1 = 75$  confined in the track is comparable to the section length  $L \sim \pi a$ . If the chain is too long to be accommodated in a single section, our interpretation of the free energy as a probability is not justified. Beyond this length, a single curved section cannot accommodate the whole chain and the chain cannot squeeze into the section due to the excluded-volume effects. Therefore, a deviation starting beyond this length is consistent with our analysis. The probability ratio  $C$  should reach a maximum in the vicinity of this length. This is consistent with our data.

#### *Conclusions.* –

We present new polymer models for Monte Carlo simulation which work well for our purpose. In particular, they have the advantage of efficient changes of the polymer conformation in restricted geometries due to the variable range character of bond lengths and of jump distances.

We have investigated the curvature effect on a flexible polymer confined in a thin box. We have plotted the ratio of probability  $C$  finding a polymer between in a curved region and in a flat region as a function of chain length  $N$ . For the ideal chains, our results agree quantitatively with the prediction of the analytic theory. We also observe a similar curvature effect on excluded-volume chains whose lengths shorter than the length of the curved section of the box.

Our simulations only cover the linear region of  $C$  as a function of chain length  $N$ , due to the limitation of our computer power for the case of model-I and due to restriction of geometrical scale of confinement for the case of model-E. However, our results may still be useful under present circumstances where there is no experimental data for either ideal or excluded-volume chains and there is no analytical theory for excluded-volume chains.

\*\*\*

The authors thank F. Wittel, P. Pincus and K. Kramer for useful suggestions. Part of this work was done during the stay of one of the authors (Y.Y.S.) at MRL UCSB.

## REFERENCES

- [1] CASASSA E.F., *Polym. Lett.*, **5** (1967) 773.
- [2] DAUD M., and DE GENNES P.G., *J. Phys. (Paris)*, **38** (1977) 85.
- [3] BROCHARD F. and DE GENNES P.G., *J. Chem. Phys.*, **67** (1977) 52.
- [4] BROCHARD-WYART F. and RAPHAEL E., *Macromolecule*, **23** (1990) 2276.
- [5] KREMER K. and BINDER K., *J. Chem. Phys.*, **81** (1984) 6381.
- [6] MILCHEV A., PAUL W. and BINDER K., *Macromol. Theory Simul.*, **3** (1994) 305.
- [7] HAGITA K. and TAKANO H., *J. Phys. Soc. Jpn.*, **68** (1999) 401.
- [8] DE GENNES P-G., *Scaling Concepts in Polymer Physics*, (Cornell University Press, Ithaca) 1979.
- [9] WALL F.T. and CHIN J.C., *J. Chem. Phys.*, **66** (1977) 3066.
- [10] KUMAR S.K., VACATELLO M. and YOON D.Y., *J. Chem. Phys.*, **89** (1988) 5206.
- [11] YAMAN K., PINCUS P., SOLIS F. and WITTEN T.A., *Macromolecules*, **30** (1997) 1173.
- [12] DOTERA T. and SUZUKI Y.Y., *Phys. Rev. E*, **61** (2000) 5318.
- [13] EISENRIEGLER E., HANKE A. and DIETRICH S., *Phys. Rev. E*, **54** (1996) 1134.
- [14] PRESS W.H., TEUKOLSKY S.A., VETTERLING W.T. and FLANNERY B.P., *Numerical Recipes in C*, (Cambridge University Press, Cambridge) 1988.